Supplementary information

Improved Efficiency of Large Area Cu(In,Ga)Se_2 Solar Cell by Non-toxic Hydrogen-Assisted Solid Se Vapor Selenization Process

Tsung-Ta Wu[1,2], Fan Hu[1,2], Jyun-Hong Huang[2,3], Chia-ho Chang[2], Chih-chung Lai[1], Yu-Ting Yen[1], Hou-Ying Huang[4], Hwen-Fen Hong[4], Zhiming M. Wang[5], Chang-Hong Shen[2*], Jia-Min Shieh[2*], and Yu-Lun Chueh[1*]

[1] Department of Materials Science and Engineering, National Tsing-Hua University, Hsinchu 30013, Taiwan

[2] National Nano Device Laboratories, No.26, Prosperity Road 1, Hsinchu 30078, Taiwan

[3] College of photonic and Institute of Imaging and Biomedical Photonics, National Chiao Tung University, Taiwan

[4] Institute of Nuclear Energy Research Atomic Energy Council, No. 1000, Wenhua Rd., Jiaan Village, Longtan Township, Taoyuan Country, Taiwan.

[5]State Key Laboratory of Electronic Thin Films and Integrated Devices, University of Electronic Science and Technology of China, Chengdu 610054, P. R. China

[*]E-mail: jmshieh@ndl.narl.org.tw, chshen@ndl.narl.org.tw, and ylchueh@mx.nthu.edu.tw

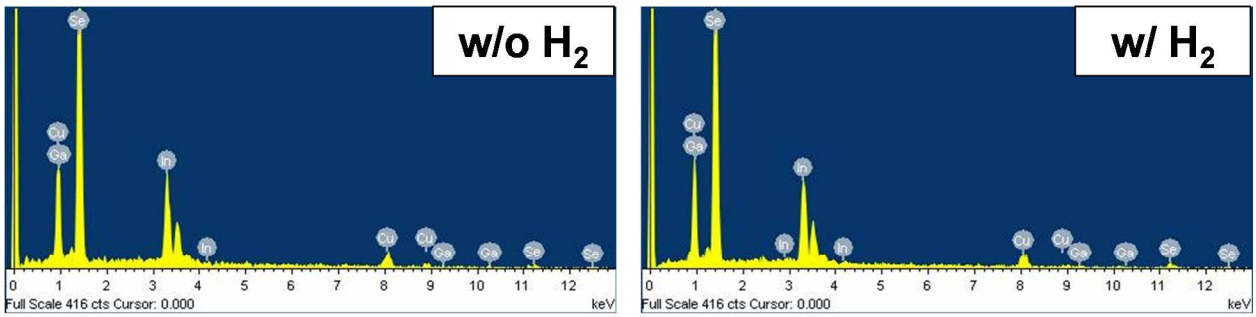

Sample #	Cu (at%)	In (at%)	Ga (at%)	Se (at%)	CGI Ratio	GGI Ratio
w/o H_2 (0% H_2)	22.6	24.6	2.8	50.0	0.83	0.10
w/ H_2 (5% H_2)	21.6	25.5	3.4	49.5	0.75	0.12

Figure S1 EDS quantitative results for CIGS thin films after the non-toxic hydrogen-assisted Se vapor selenization process and the selenization in the N_2 ambeint. Both samples exhibit the identical stoichiometric atomic composition ratio of bulk volume [Cu/(In+Ga)~0.8, Se~50 %].

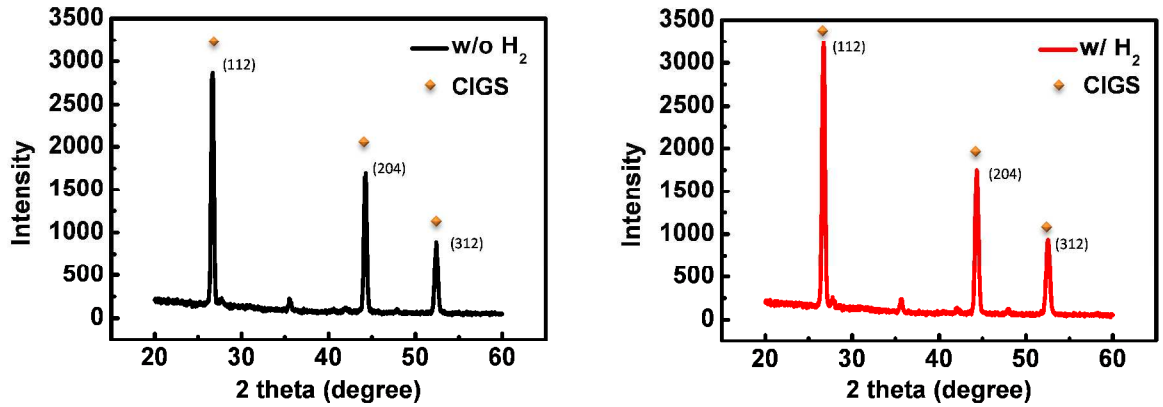

Figure S2 X-ray sspectra for CIGS thin films after the non-toxic hydrogen-assisted Se vapor selenization process and the selenization in the N_2 ambeint. Btoth samples exhibit good crystallinity and strong (112) and (220)/(204) preferred orientation from GIXRD results.

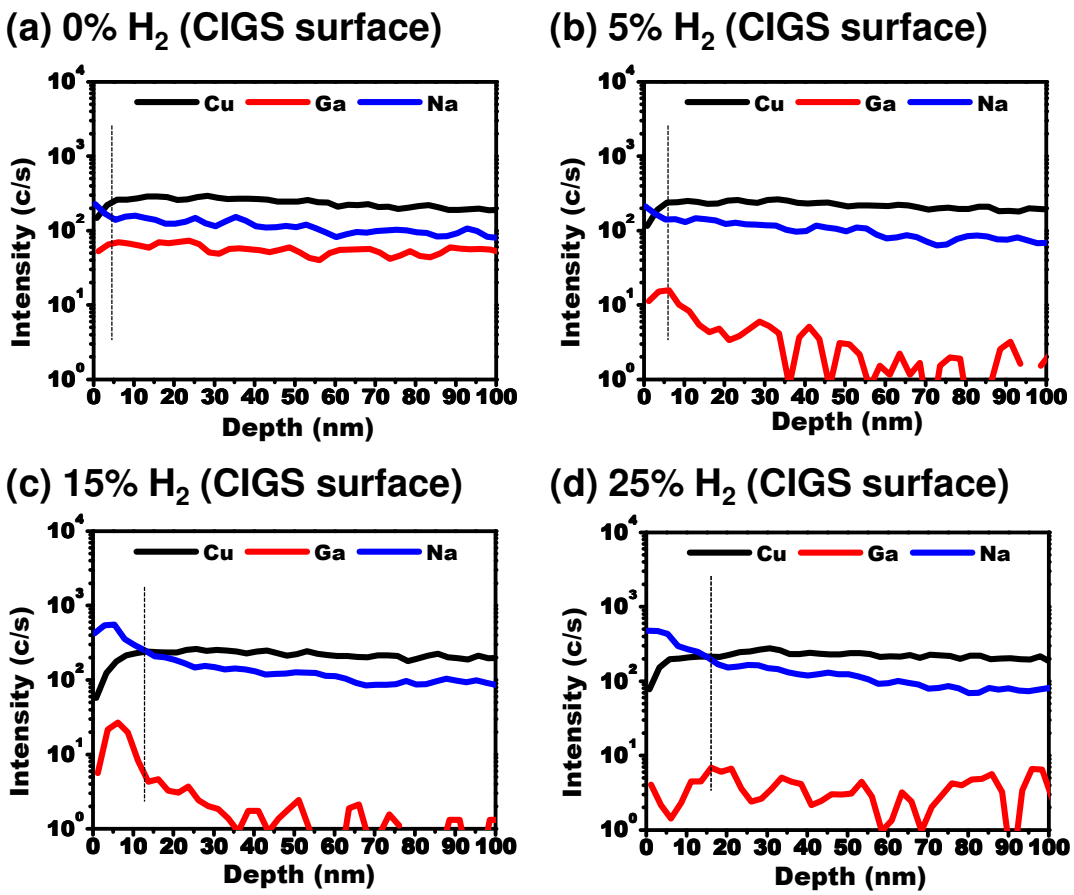

Figure S3 Near surface SIMS depth profiles of CIGS surface for (a) pure N_2 ambient (0% H_2), (b) 5 % H_2, (c) 15 % H_2, and (d) 25% H_2, respectively.

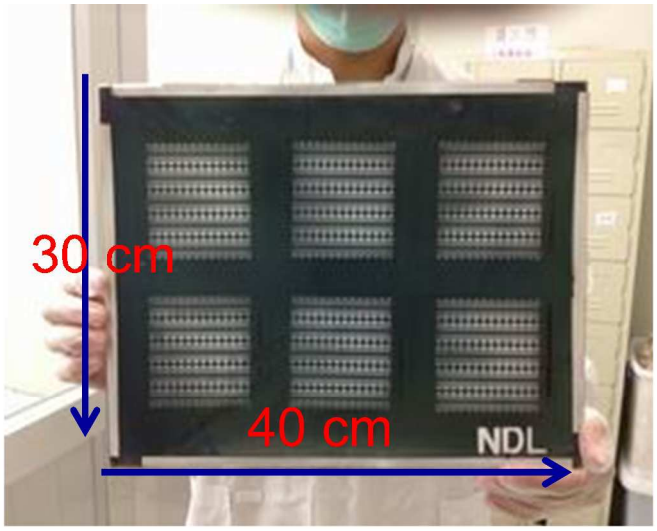

Figrue S4 CIGS solar cell panels (30 cm× 40 cm)

Emitting Mechanisms

Radiative processes of CIGS thin films may include band-impurity (BI) and donor-to-acceptor (DAP) transitions. The emission spectra of these three peaks are fitted by BI (CB to A1), DAP1 (D1 to A1), and DAP2 (D1 to A2) recombination models. The extracted donor level and acceptor level are consistent with shallow A1- mostly Cu vacancy (V_{Cu}), shallow D1 – mostly Se vacancy (V_{Se}), and deep A2 – mostly O occupied Se vacancy (O_{Se}) at the energies of (E_v +0.03 eV), (E_c -0.08 eV) and (E_v +0.12 eV), respectively[1,2]. I_{BI} and I_{DAP1} are relative intensities of BI and DAP1 transitions where I_{DAP1} / I_{BI} positively relative to intensity of PL mapping. The ratios increase with H_2 ratios represent less existence of deep level defects.

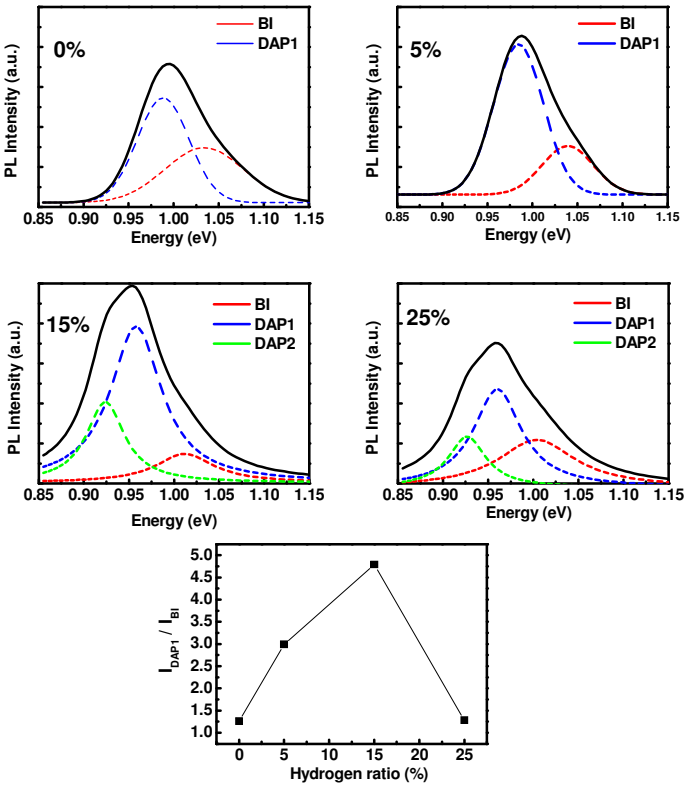

Figure S5 Low temperature PL of I_{DAP1} to I_{BI} relative ratio corresponds to PL mapping intensity.

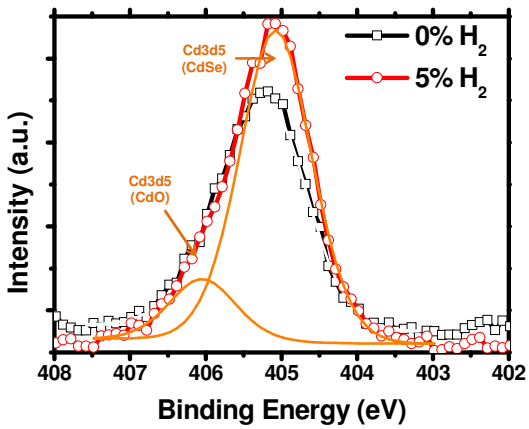

Figure S6 XPS bonding characterization of samples with and without hydrogen-assisted Se vapor selenization. The Cd-Se bonding intensity increases in hydrogen assisted selenization sample, which is due to wider copper poor region lead to more cadmium ions diffuse into CIGS thin films.

Carrier density measurements of the CIGS film after the hydrogen-assisted selenization process by DLCP

To certify the cell performance enhancement of surface sodium accumulation effect, DLCP is used to verify carrier density in high frequency response range[3]. Drive level capacitance profiling (DLCP, iHR550) is a useful technique for studying amorphous and polycrystalline semiconductors. This technique directly yields the density of states within the band gap of the semiconductor, as a function of both energy and of spatial position, requiring knowledge only of the semiconductor dielectric constant (ε). It also provides a much more accurate assessment of the free carrier density in the film than the C-V method[4]. As figure S5 shown, in hydrogen enhanced selenized (15% H_2) sample, the N_{DL} (drive level density) reaches as high as 3.0 x 10^{16} cm^{-3}, three times larger than reference sample (0% H_2) with drive level density about 1.0 x 10^{16} cm^{-3}. In previous results[5,6], carrier density enhancement can be thought as the merit of Na effect in CIGS film, and hydrogen enhanced selenization treatment does has the same effect.

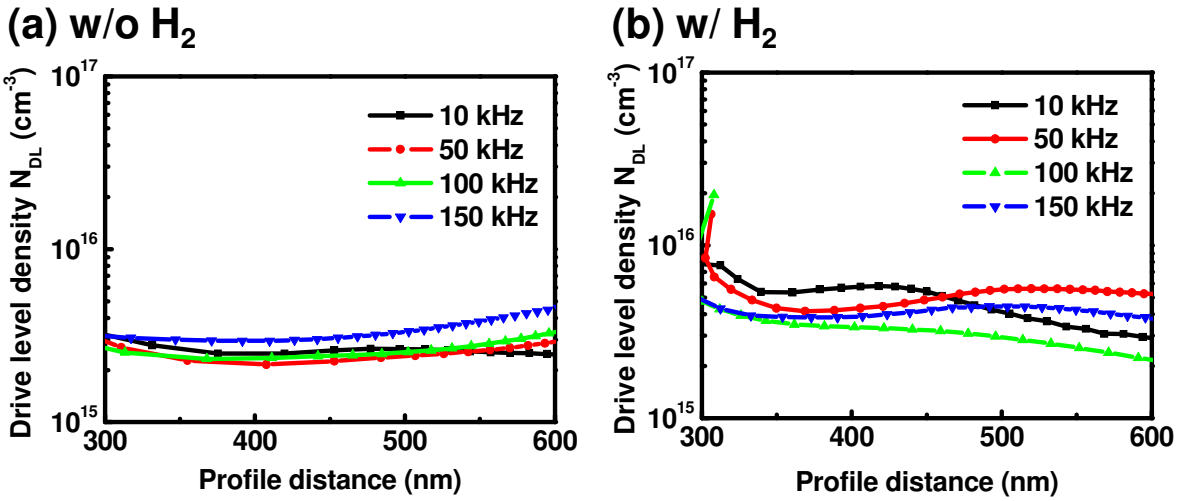

Figure S7 DLCP of carrier concentration measurement for (a) without and (b) with hydrogen-assisted Se vapor selenization. Higher drive level density (3.0 x 10^{16} cm^{-3}) represents higher carrier concentration, which is measured from the hydrogen assisted selenization sample

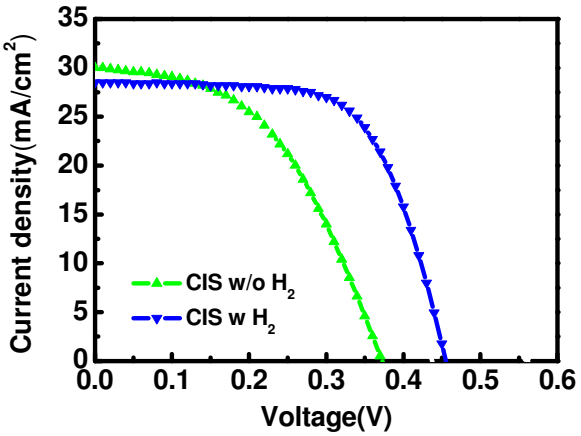

	Cond.	η (%)	FF	V_{oc} (mV)	J_{sc} (mA/cm^2)	R_{sh} (Ω/cm^2)	R_s (Ω/cm^2)	J_0 (A/cm^2)
CIS	w/o H_2	5.3	48.0	370.0	30.0	60.0	3.1	7.0E-6
	w/ H_2	8.5	64.5	460.0	28.5	849.0	1.7	1.0E-6

Figure S8 J-V measurements of $CuInSe_2$ solar cells after the hydrogen-assisted Se vapor selenization process.

References

1. Ishizuka, S.; Yamada, A.; Islam, M. M.; Shibata, H.; Fons, P.; Sakurai, T.; Akimoto, K.; Niki, S. Na-induced Variations in the Structural, Optical, and Electrical Properties of Cu(In,Ga)Se_2 Thin Films J. Appl. Phys. 2009, 106, 034908.
2. Cheng, T. -H. Photoluminescence Characterization and Passivation of CIGS Absorber ECS Transactions 2011, 33, 191 - 197.
3. Johnson, P. K.; Heath, J. T.; Cohen, J. D.; Ramanathan, K.; Sites, J. R. A Comparative Study of Defect States in Evaporated and Selenized CIGS(S) Solar Cells Prog. Photovoltaics 2005, 13, 1 - 8.
4. Heath, J. T.; Cohen, J. D.; Shafarman, W. N. Bulk and Metastable Defects in $CuIn_{1-x}Ga_xSe_2$ Thin Films Using Drive-level Capacitance Profiling J. Appl. Phys. 2004, 95, 1000 - 1010.
5. Keyes, B. M.; Hasoon, Falah,; Dippo, Pat.; Balcioglu, A.; Abulfotuh, F. Influence of Na on the Electro-optical Properties of Cu(In,Ga)Se_2 26th IEEE Photovoltaic Spec. Conf. 2007, 479 - 482.
6. Ersleva, P. T.;, Lee, J. W.; Shafarman, W. N.; Cohen, J. D. The Influence of Na on Metastable Defects Kinetics in CIGS Materials Thin Solid Films 2009, 517, 2277 - 2281.